

# TSIS EXPERIENCES WITH ISS JITTER FROM INCEPTION TO ON-ORBIT OPERATION

Patrick Brown and Andrew Engelmann\*

The TSIS instrument has been measuring solar irradiance on a continual basis since January 2018 as an external payload on the ISS. In 2014 when TSIS was directed to fly on the ISS, the jitter environment was highly uncertain, so TSIS designed a robust gimballed pointing system that showed excellent disturbance attenuation throughout the design, test, and on-orbit phases of the program. This paper discusses how TSIS accounted for this uncertain jitter environment throughout the life of the program.

TSIS was able to measure the ISS jitter during commissioning and determined that it was a relatively benign environment less than 4 arcseconds  $1\sigma$  at low frequencies ( $<0.5$  Hz). More importantly, the measured pointing performance of TSIS was consistently found to be 4 arcseconds  $1\sigma$ , which easily satisfied the jitter requirement of 60 arcseconds  $1\sigma$ .

## INTRODUCTION

The Total and Spectral Solar Irradiance Sensor (TSIS) measures total and spectral solar irradiance in order to continue the multi-decade-long records of these important physical quantities. TSIS was installed onto Site 5 of ELC-3 on the International Space Station (ISS) in December 2017 and has been operating continuously since then.

In order to collect its scientific measurements, TSIS requires precision solar pointing every orbit that is accomplished via a 2-axis gimballed pointing system. When the ISS was initially selected in 2014 as the accommodation for TSIS, the effect of ISS base motion jitter was a significant concern that influenced the entire development process from inception to on-orbit operation.

This paper begins by providing a brief overview of the TSIS instrument and how it performs solar pointing from the ISS. Next, an overview of the ISS jitter environment is presented to convey the challenges associated with ISS jitter. Then, the pointing system hardware architecture is described that provides robust performance in the presence of the uncertain jitter environment. The control design approach is described next, including modeling, simulation, and analysis. Then, testing and verification of the pointing controller is described. Lastly, on-orbit results are presented that include measurements of ISS background jitter and TSIS pointing performance. Concluding remarks complete the paper.

---

\*Laboratory for Atmospheric and Space Physics at the University of Colorado  
1234 Innovation Dr, Boulder CO 80303.

## TSIS INSTRUMENT OVERVIEW

TSIS is a NASA instrument designed, built, and operated by the Laboratory for Atmospheric and Space Physics (LASP) at the University of Colorado that continues the 39-year-long record of total solar irradiance (TSI) and the 15-year-long record of spectral solar irradiance (SSI). Both TSI and SSI are critical to long-term climate monitoring. TSI is measured by the Total Irradiance Monitor (TIM), and SSI is measured by the Spectral Irradiance Monitor (SIM). These two sensors comprise the TSIS instrument along with the pointing system that will be discussed in this paper.

TSIS was launched to the ISS on December 15, 2017 aboard a SpaceX Falcon 9 rocket in the Dragon trunk. It was then installed on the zenith side of the ISS at Site 5 of Express Logistics Carrier (ELC) 3 as shown in Figure 1 below. After robotic arm installation, the TSIS deployment system rotated the gimbaled instrument suite into its operational position above the ELC. TSIS's operational position above the ELC allows for a hemispherical view of the sky and solar viewing every orbit during its 5-year mission.

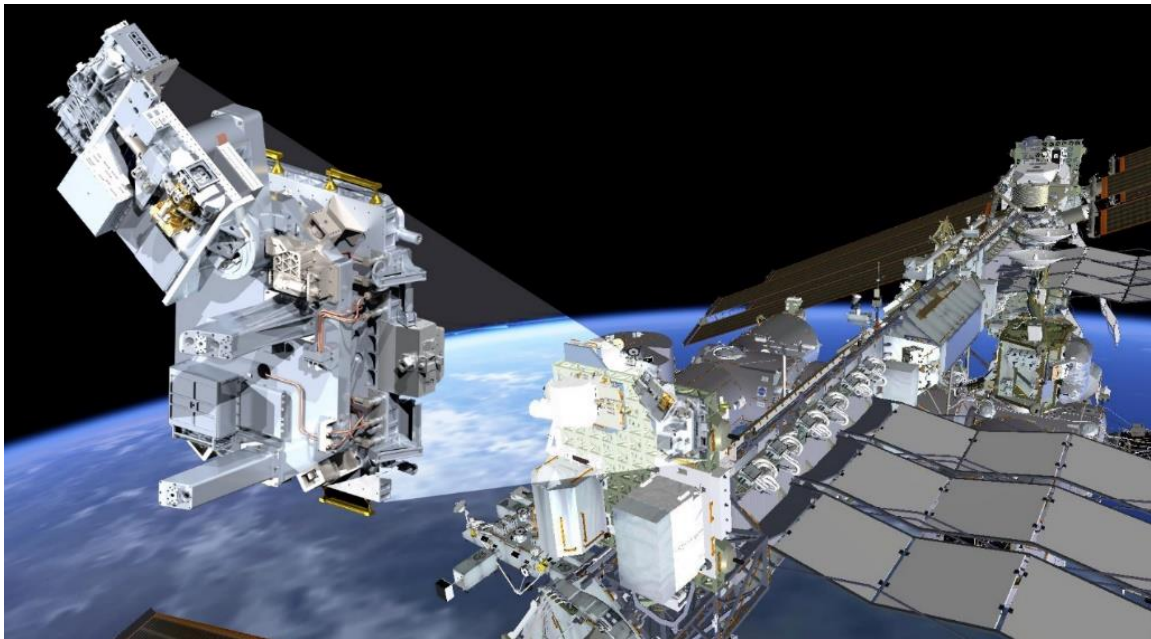


**Figure 1: TSIS Instrument Shown at ELC 3-5 Mounting Location on ISS**

In order to perform solar measurements, TSIS must be pointed directly at the sun for 40 minutes per orbit with less than 60 arcseconds  $1\sigma$  precision while subject to movement by the nadir-pointed ISS. To decouple the TSIS instruments from ISS motion, the Thermal Pointing System (TPS) was developed. The TPS provides both thermal and pointing control for the TSIS scientific sensors; however, this paper is only concerned with the pointing aspects of the TPS.

### Gimbal Motion Profile

The TPS follows approximately the same motion profile every orbit as shown in the flight data in Figure 2 below. The azimuth axis provides the primary motion of the gimbal over the course of the orbit as it tracks the sun overhead from sunrise to sunset from  $+110^\circ$  to  $-110^\circ$  at a rate of approximately  $4^\circ/\text{min}$ . The elevation axis accounts primarily for variations in the solar beta angle that varies periodically every 60 days with annual maxima/minima of  $\pm 74^\circ$ . Additionally, both axes account for motion due to static and dynamic offsets of the ISS flight attitude relative to the Local

Vertical-Local Horizontal reference frame. Finally, the TPS points to zenith during every eclipse to support dark space measurements.

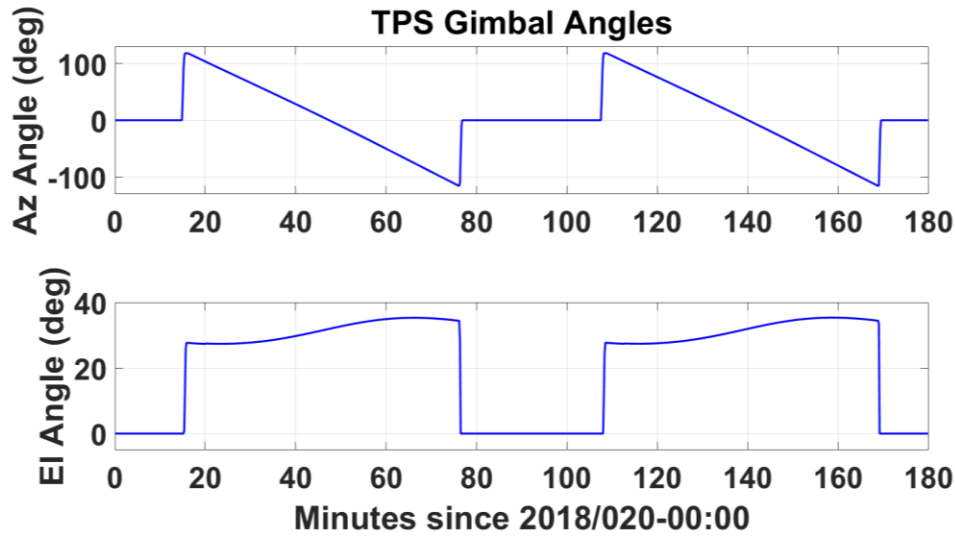


Figure 2: Typical TPS Gimbal Motion Profile

## ISS JITTER ENVIRONMENT

When TSIS was directed in 2014 to fly on the ISS, the ISS background jitter environment was poorly understood from a pointing perspective that led to significant uncertainty in the effect that base motion-induced jitter would have on TSIS pointing. In particular, very little information was available about ISS jitter and most of it focused on ISS vibration as it related to structural safety at non-ELC locations rather than to pointing performance for external payloads on ELCs. For instance, no measurements of ISS angular jitter existed at external payload sites to help guide future payloads, and no procedural mechanism existed (or will exist) to manage ISS jitter.

Whereas a free-flyer spacecraft will typically examine the effects of all significant disturbance sources (i.e., microvibrations) on all pointing boresights to ensure mutual compatibility, the ISS does not perform this type of pointing sensitivity analysis. Instead, the only jitter-related interface information from the ISS is their “suggested on-orbit random vibration (OORV)” environment that payloads use to evaluate structural loads and is therefore a conservatively large estimate of base motion for jitter analysis. However, because no other information or guidance existed in 2014, TSIS used the suggested OORV to evaluate jitter during the design and analysis phases of the program.

As an aside, since the TPS was designed in 2014, several ELC-mounted payloads, including the Optical Payload for Lasercomm Science (OPALS)<sup>1</sup>, Stratospheric Aerosol Gas Experiment III (SAGE III)<sup>2</sup>, and now TSIS, have been able to successfully measure the jitter environment at their specific ELC mounting locations. The TSIS jitter measurements will be discussed later in this paper. It is anticipated that these new measurements will reduce the uncertainty in the ISS jitter environment for future payloads. However, due to the large physical scale of the ISS and the dynamic configuration of payloads, modules, and visiting vehicles, future instrument payloads will still be proceeding at risk, because the jitter environment could change spatially depending on mounting location and temporally as the station configuration evolves.

## TSIS POINTING SYSTEM

The TPS is based on a two-axis, elevation over azimuth gimbal that points the instrument optical bench (including the SIM and TIM sensors) relative to the TSIS base plate as shown in Figure 3 below. The optical bench dimensions are 1.0 m wide by 0.9 m deep by 0.38 m tall with a moving mass of 83 kg and a rotational inertia of 10.2 kg•m<sup>2</sup> about the azimuth axis and 3.8 kg•m<sup>2</sup> about the elevation axis.

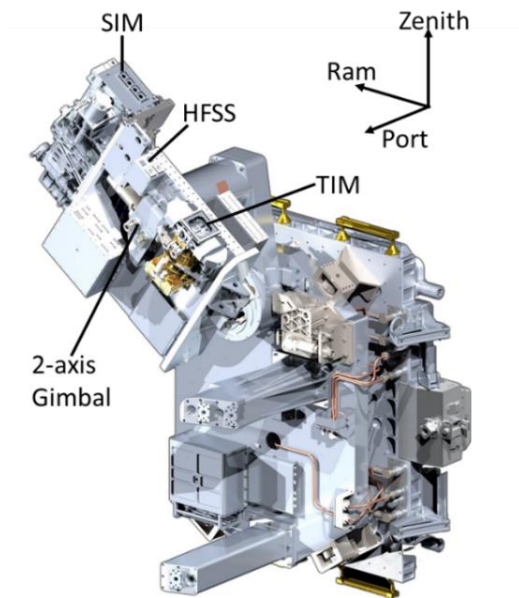


**Figure 3: TSIS Instrument Components**

Because such large uncertainty existed regarding the ISS jitter environment, the TPS was designed to be robust to this uncertainty by including two novel hardware features: 1) brushless DC (BLDC) gimbal motors for actuation, and 2) High-rate Fine Sun Sensors (HFSS) for sensing.

BLDC motors were selected instead stepper motors, which are commonly used by NASA missions, due to the numerous advantages they offer compared to stepper motors, including: continuous torque command authority, minimal self-induced jitter, increased active control bandwidth, and structural separation from base motion. All of these factors combine to provide a significant increase in base disturbance attenuation compared to stepper motors. In particular for TSIS, the BLDC motors provide significant passive attenuation at higher frequencies ( $>5$  Hz) and active attenuation at lower frequencies ( $<5$  Hz)<sup>3</sup>. The BLDC actuators consist of the following components: BLDC direct-drive motors, 2-speed (1x, 16x) resolvers, brakes, twist capsules for signal/power feed-thru, and output duplex pair bearings.

The HFSS provides direct measurements of solar offset angles of the TSIS boresight and is used for both feedback control and for knowledge. The HFSS uses a quad-diode sensor and responds linearly over a  $\pm 2.5^\circ$  field of view (FOV) in two orthogonal with measured precision of 1 arcsecond  $1\sigma^4$ . It produces data at 200 Hz, which allows for its use in feedback control systems for not only slow-speed tracking but also for high-speed stabilization of jitter disturbances. Using only the HFSS for control feedback greatly simplified the control architecture by eliminating the need for a complex, multi-sensor approach including inertial reference units. The high rate also provides highly granular temporal knowledge for examining jitter.

Additionally, the TPS includes a dedicated control electronics box that consists of the drive electronics, a flight computer, power handling, and interfaces to the various TPS actuators and sensors. Finally, as already mentioned, the TPS includes a deployment system that rotates the optical bench to its operational position and holds it rigidly in place.

## TPS CONTROL DESIGN AND ANALYSIS

In order to use the actuators and sensors together in a robust manner to mitigate base motion jitter, the closed-loop pointing controller was modeled, designed, and simulated using classical, robust techniques<sup>5</sup>.

### Modeling of the TPS Control System

A high-fidelity, non-linear dynamic model of the TPS was developed that included dynamic models of the compensators, actuators, sensors, and TPS structure as shown in the high-level Simulink/SimMechanics block diagram in Figure 4 below. Linearized versions of the model were used for control design purposes, and the full non-linear model was used to simulate the response of the TPS to ISS base motion jitter.

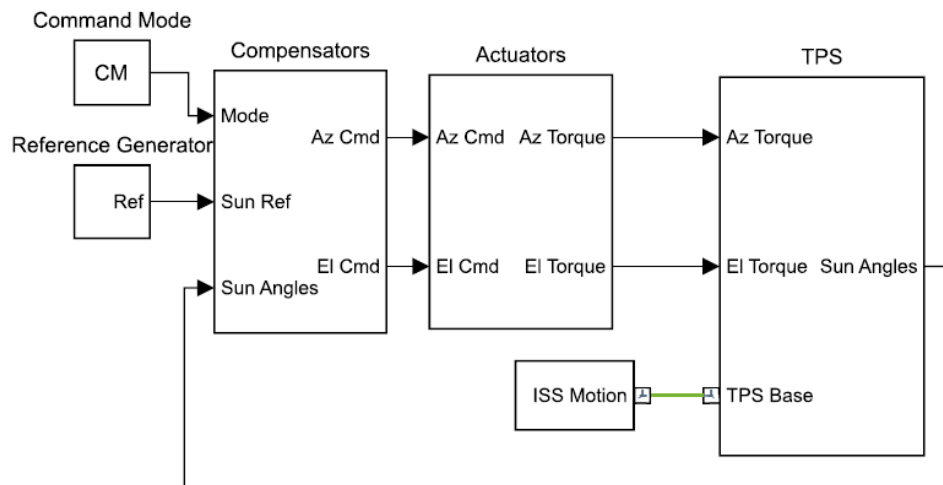


**Figure 4: TPS High-Level Simulink Block Diagram**

The model was arranged as a typical feedback controller, starting with commands on the left that propagate through compensators that drive plant dynamics that affect the control variables (sun angles) that are ultimately fed back to the compensator to complete the loop. The closed-loop compensation was digitally implemented independently for each axis at 200 Hz to correctly represent how it would be later implemented in flight software. In order to examine the effect of ISS jitter, the TPS dynamics block was connected at its base to an ISS prescribed motion block that could be configured to represent the suggested OORV environment.

To examine possible interactions of the TPS structure with ISS jitter, the four lowest frequency structural modes were included in the model as additional degree of freedoms with stiffness and damping chosen to match the mode shapes and frequencies with those from the high-fidelity TSIS finite element model.

Model accuracy was ensured by incorporating parameter updates as the test program proceeded and new parameter measurements were taken. More details will be provided later in the Frequency Response Testing section of this paper.

## TPS Controller Design

The pointing system controller was designed to minimize the impact of base motion jitter on pointing performance. A classical proportional-integral-derivative (PID) plus filter controller structure was chosen for the compensators for its simplicity and well-established control characteristics. The PID compensator is shown below in Equation (1) in continuous time format, where  $s$  is a complex variable (generalized frequency),  $K_p$  is the proportional gain,  $K_i$  is the integral gain, and  $K_d$  is the derivative gain. An additional low pass filter, with cutoff frequency,  $\omega_f$  is included to limit the amount of high frequency noise introduced by the derivative term.

$$C(s) = K_p + K_i \frac{1}{s} + \frac{K_d s}{s/\omega_f + 1} \quad (1)$$

The primary control design objective was to maximize disturbance attenuation (both magnitude and bandwidth), while maintaining adequate stability margins. Because of the correlation between the disturbance transfer function and the open-loop transfer function, the design goals were able to be simultaneously evaluated with the open-loop transfer function.

Classical control design techniques were used to shape the open-loop transfer function for each axis, which consisted of the controller and the plant. The open-loop transfer function Bode plot (magnitude and phase), for both the Azimuth (Laz) and Elevation (LeI) gimbal motors, is shown in Figure 5 below. The poles and zero of the controller were selected to shape the open-loop transfer function to achieve the desired performance and stability properties. In particular, the integrator pole added low frequency gain reducing steady-state tracking errors, while the zero introduced by the derivative control was adjusted to add phase near the cross-over frequency, which increased phase margin and damping (lowered overshoot). The additional low pass filter increased roll-off at higher frequencies, which limited the effect of high frequency noise injected into the loop. Finally, the gain was adjusted to achieve a cross-over frequency of 2.5 Hz that reduced the effect of jittery over-control in the current signals. The design of the flight controllers for both gimbal motors resulted in phase margins of 54 deg, gain margins of 15 dB, and bending mode margins of 22 dB (at the lowest mode frequency of 16 Hz).

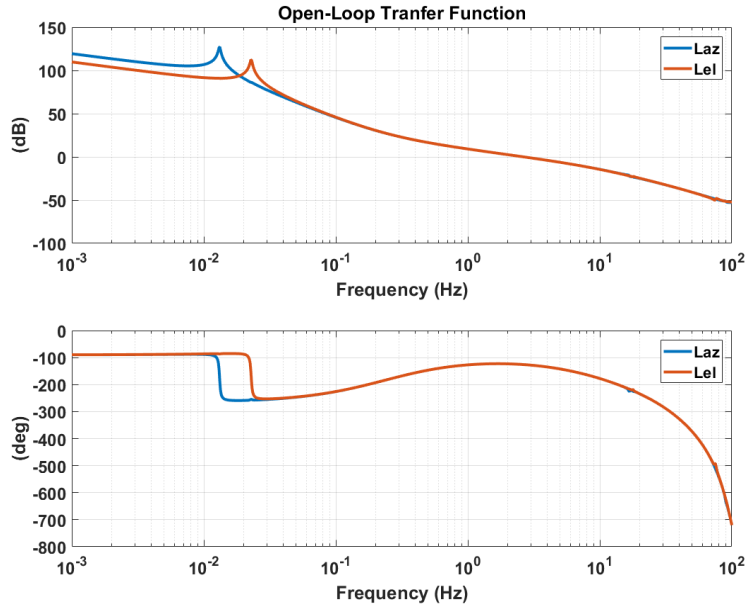
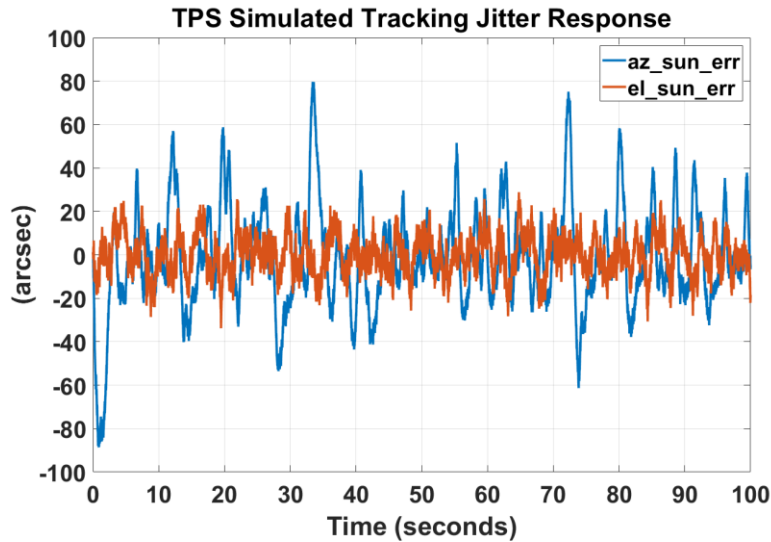


Figure 5: TPS Controller Open-Loop Frequency Response Design



## Simulation and Analysis

The main purpose of the pointing control simulation was to evaluate the effect of ISS base motion on TPS pointing jitter. To perform the simulations, the ISS suggested OORV levels were translated from the frequency domain into time series values that were input one axis at a time to the TPS Base model as previously shown in Figure 4. Example results of this simulation are shown in Figure 6 below that indicate the azimuth (az\_sun\_err) and elevation (el\_sun\_err) tracking errors (aka jitter) when subject to the ISS suggested OORV.



**Figure 6: Simulated Solar Tracking Performance Using Suggested OORV Jitter**

1-sigma values of the simulated tracking performance are shown below in Table 1 for input jitter along the three axes. The root sum squared (RSS) line at the bottom of the table represents a worst case jitter scenario and is the estimate of tracking performance if jitter were present in all three input axes simultaneously. Even in the worst case scenario, the simulated tracking errors of 31.8 arcseconds  $1\sigma$  provided 47% margin below the 60 arcseconds  $1\sigma$  requirement.

**Table 1: Simulated Solar Tracking Errors Using Suggested OORV Jitter**

Jitter Input Axis	(arcsec $1\sigma$ )	
	Az	El
X	11.5	3.9
Y	23.6	9.1
Z	18.0	7.3
<b>RSS</b>	<b>31.8</b>	<b>12.3</b>

Parametric sensitivity analyses were also performed that varied most important parameters, including: structural damping, CG offset of the pointing platform, sun sensor noise, pointing platform inertia, motor friction, motor winding resistance, control loop delay, on-orbit jitter level, and jitter input axis. The analysis showed that the system tracking performance was insensitive to most parameters, except for the CG offset, the low frequency structural modes, and the ISS jitter magnitudes. The actual ISS jitter magnitudes were beyond the control of the TSIS program, but this analysis resulted in tight procedural control of the CG location and the low frequency structural modes.

## TPS TESTING AND VERIFICATION

Two types of testing were performed to evaluate the TPS pointing performance from a jitter perspective: 1) frequency response testing, and 2) solar tracking testing.

### Frequency Response Testing

Frequency response measurements of the TPS control loop were performed numerous times (10+) throughout the integration and test program as the hardware and software configurations evolved. These tests provided direct measurements of the system dynamics including the compensator and plant, which provided information for model correlation, verification of control stability margins, and a direct measurement of the disturbance rejection capability. It was extremely advantageous to perform direct measurements of these important quantities for the TPS, especially given how uncommon it is to be able to perform similar measurements for a spacecraft attitude control system.

The frequency response measurements were performed by injecting a sinewave into the reference, measuring the angles and commanded current, and then calculating the ratios of magnitude and phase between appropriate points in the loop. After measurements were performed, the results were compared to the model, adjustments were made to the PID coefficients in the model to achieve the desired effects, and the updated PID coefficients were used for a subsequent frequency response measurement of the hardware. Although time consuming, this iterative approach allowed for highly accurate adjustment of the pointing controller and ensured that the model matched the hardware. And because the model was tightly correlated with the actual hardware, it was then possible to use it to predict the TPS response to the suggested OORV environment with high confidence.

To understand the effect of base motion jitter on pointing performance, it is helpful to examine the “input” disturbance transfer function as shown in Figure 7 below. The plot shows both the modeled and the measured responses, both of which show excellent agreement and robust, broadband disturbance attenuation.

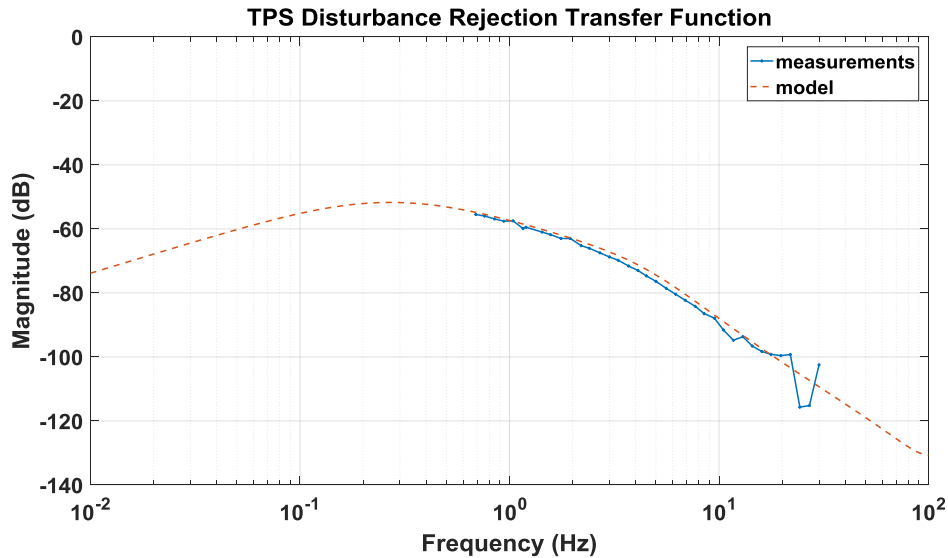


**Figure 7: Measured Input Disturbance Transfer Function**



## Solar Tracking Testing

Although it was not possible to directly test the response of the TPS to base motion jitter, it was possible to measure the steady-state solar tracking errors (self-induced jitter) for the azimuth axis during closed-loop, flight-like solar tracking conditions that included  $4^\circ/\text{min}$  constant-rate ISS base motion simulated by a rotational stage and a fixed solar simulator as shown in Figure 8 below.

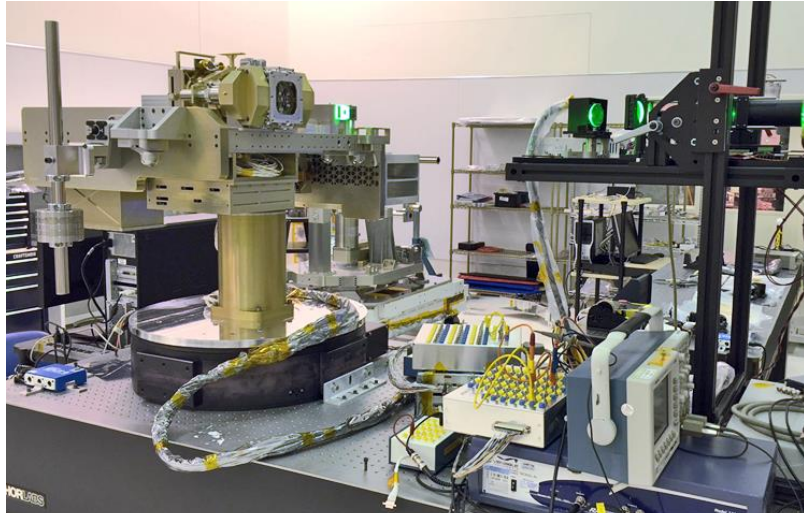


**Figure 8: TPS Solar Tracking Test Configuration**

Results of this test are shown in Figure 9 below as measured by the HFSS. The HFSS errors are shown in magenta, and an independent angular measurement was provided by a ring laser gyro (RLG) shown in blue that follows the HFSS errors throughout the dataset. The measured HFSS error is 6 arcseconds  $1\sigma$  over this dataset, and the RLG error is slightly less at 4 arcseconds  $1\sigma$  because it is only measuring the mechanical motion and not the optical noise from the solar stimulus. This dataset was of high importance during the test program because it demonstrated that the BLDC actuators were capable of providing very low self-induced jitter compared to the 60 arcseconds  $1\sigma$  requirement.

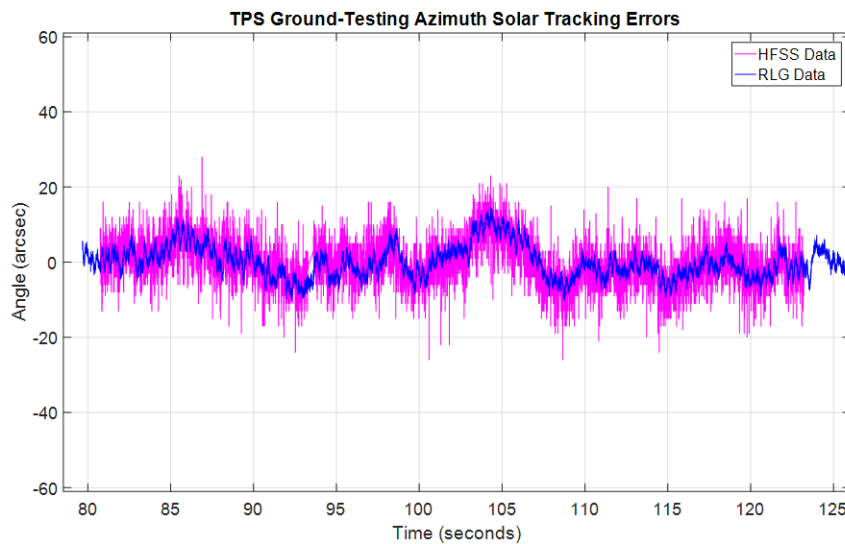


**Figure 9: Solar Tracking Errors during Ground Testing**

## ON-ORBIT JITTER MEASUREMENTS AND POINTING PERFORMANCE

After TSIS was installed onto Site 5 of ELC 3 in late December 2017, several weeks of commissioning ensued that allowed the TSIS team to finally understand the ISS jitter environment and the TPS pointing performance.

### Measurements of ISS Jitter

Measurements of the ISS background jitter were taken very early in the commissioning program in order to provide a baseline against which the TSIS pointing performance could be compared. ISS jitter measurements were performed by positioning the gimbal in a stationary position that allowed for transits of the sun through the HFSS FOV. Because of the gimbal orientation of TSIS on the ISS, the solar transits resulted in nearly linearly motion of the sun along the azimuth axis of the HFSS due to ISS pitch motion and sinusoidal motion along the elevation axis due to the ISS yaw offset.

Six high-rate (200 Hz) jitter observations and 62 opportunistic low-rate observations were performed, and all data sets showed good agreement with each other<sup>5</sup>. HFSS data was captured in telemetry for subsequent ground processing. After data was received on the ground, rigid-body motion of the ISS was removed by applying a linear fit to the azimuth axis and a quadratic fit to the elevation axis that resulted in residuals that indicated the ISS jitter as shown in Figure 10 below from HFSS-A.

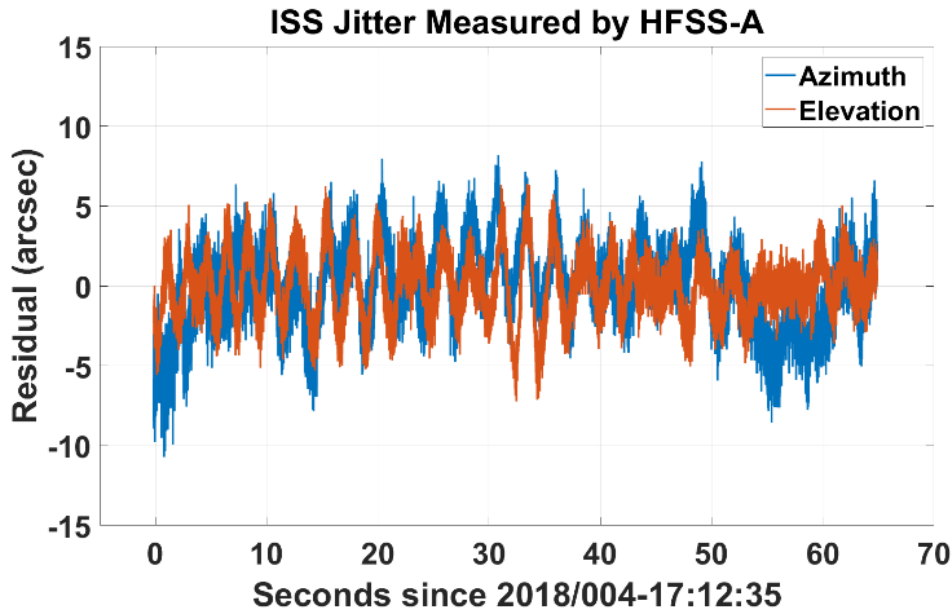


**Figure 10: Time Series of ISS Jitter Measured by HFSS at 200 Hz**

Several characteristics were readily apparent in this dataset and all the others:

1. The magnitude of the jitter was relatively small with magnitudes less than 4 arcseconds  $1\sigma$
2. The HFSS measurement precision of 1 arcsecond  $1\sigma$  was visible as noise on the signal and was not indicative of actual ISS jitter motion
3. The frequency of the jitter was relatively low ( $<0.5$  Hz)

Of course, these measurements were taken over a very short time window in January 2018 and at the TSIS location on ELC 3-5, but they were consistent with the similar OPALS measurements

from 2015-2016 on ELC-1<sup>1</sup>. These results are encouraging for payload developers, because they indicate a relatively benign jitter environment, which could greatly reduce the need for sophisticated jitter mitigation solutions. For example, the Climate Absolute Radiance and Refractivity Observatory (CLARREO) Pathfinder mission that will fly on the ISS in 2023 was able to descope a costly inertial measurement unit from the design in part due to these results.

### TPS Pointing Performance

The final, and arguably most important, aspect of the TSIS jitter story was the on-orbit measurement of TPS pointing performance that provided direct verification of pointing jitter compared to the 60 arcseconds  $1\sigma$  requirement in its actual operating environment that included ISS jitter. To perform the verification, the TPS performed closed-loop solar tracking using the HFSS, and high-rate 200 Hz HFSS measurements were recorded that could reveal high-frequency pointing characteristics. A dozen of these 120 second-long, high-rate measurements were taken using both HFSSs to verify consistency between the results and to provide correlation to the 1 Hz, low-rate data that would be used to evaluate performance through the remainder of the mission.

Figure 11 below shows one of these measurements from HFSS-B that shows pointing errors of 4 arcseconds  $1\sigma$  in the azimuth axis and 2 arcseconds  $1\sigma$  in the elevation axis. This performance easily satisfied the jitter requirement of 60 arcseconds  $1\sigma$ . This data was also examined in the frequency domain, and it was determined that the frequency content of the error signals was  $<0.5$  Hz with only HFSS noise at higher frequencies. This allowed nominal 1 Hz rate to be used to evaluate pointing errors for the remainder of the mission. All of the additional high-rate and low-rate pointing measurements from throughout the flight mission are consistent with these results. This significant margin has allowed the TSIS sensors to perform their measurement without concern of pointing errors and also provides ample buffer in case the ISS jitter environment were to increase due to a change in configuration.

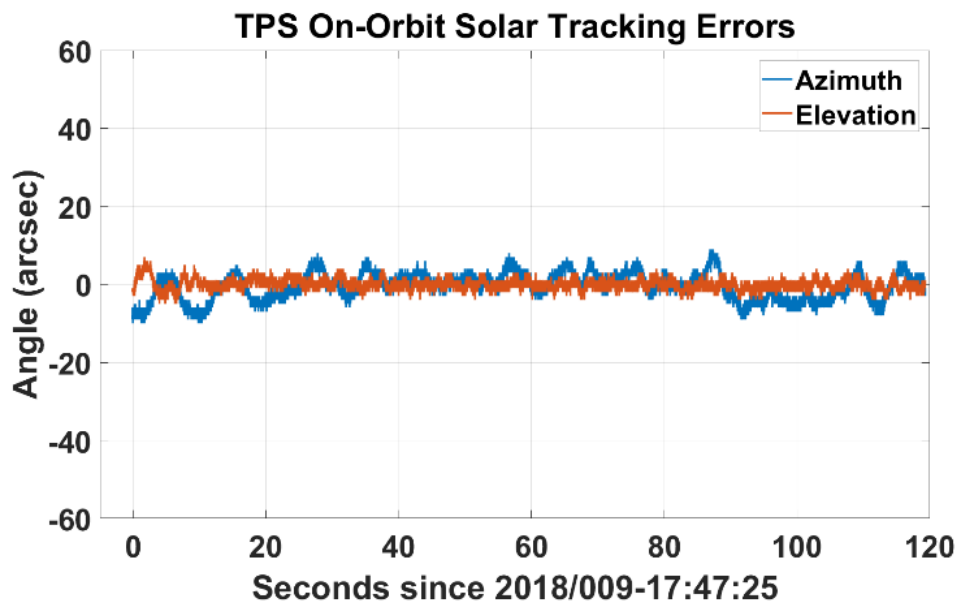


Figure 11: Typical TSIS On-Orbit Solar Tracking Errors

## CONCLUSION

The International Space Station offers an attractive platform for external payloads in many regards, but its jitter environment was poorly understood when TSIS was directed in 2014 to fly on the station. To account for this uncertainty, TSIS was designed to be robust to jitter via its hardware design that included direct-drive BLDC actuators and the HFSS, and its control design and analyses. The design analyses showed adequate margins for pointing performance that was later verified during the test phase of the program and ultimately again on-orbit.

To help quantify the uncertain ISS jitter environment, TSIS performed direct measurements using the HFSS that showed a relatively benign environment less than 4 arcseconds  $1\sigma$  at low frequencies ( $<0.5$  Hz). Most importantly, the measured pointing performance of TSIS was consistently found to be 4 arcseconds  $1\sigma$ , which easily satisfied the jitter requirement of 60 arcseconds  $1\sigma$ . Although it was undesirable to be faced with such an uncertain environment, the decision to build a pointing system that was robust to jitter clearly benefited the program by providing excellent performance.

## REFERENCES

- <sup>1</sup>Oaida, B., D. Bayard, and M. Abrahamson, “On-orbit Measurement of ISS Vibrations during OPALS Extended Mission Operations”, *2017 IEEE Aerospace Conference*.
- <sup>2</sup>Rowell, A., C. Hill, K. Leavor, A. Berner, K. Perkins, “SAGE III ISS Disturbance Monitoring Package: Observations From The First Year On Orbit”, *2018 International Space Station Research and Development Conference*.
- <sup>3</sup>Brown, P., A. Engelmann, and R. Lewis, “Use and Advantages of Direct-Drive Brushless DC Actuators for Precision Instrument Pointing of the Total and Spectral Solar Irradiance Sensor”, *Proceedings of the 44<sup>th</sup> Aerospace Mechanisms Symposium*, May 2018.
- <sup>4</sup>Brown, P., “Challenges and Solutions for Precision Solar Pointing on the ISS for the TSIS Instrument”, *2019 IEEE Aerospace Conference*.
- <sup>5</sup>Engelmann, A., “Modeling, Simulation, and Robust Design of the TSIS Pointing Controller for ISS Deployment”, *2019 IEEE Aerospace Conference*.